Cavity-Mediated Coherent Coupling between Distant Quantum Dots

Giorgio Nicolí,[1] Michael Sven Ferguson,[2] Clemens Rössler,[3] Alexander Wolfertz,[1] Gianni Blatter,[2] Thomas Ihn,[1] Klaus Ensslin,[1] Christian Reichl,[1] Werner Wegscheider,[1] and Oded Zilberberg[2]

[1]*Solid State Physics Laboratory, ETH Zürich, 8093 Zürich, Switzerland*
[2]*Institute for Theoretical Physics, ETH Zürich, 8093 Zürich, Switzerland*
[3]*Infineon Technologies Austria, Siemensstraße 2, 9500 Villach, Austria*

Scalable architectures for quantum information technologies require one to selectively couple long-distance qubits while suppressing environmental noise and cross talk. In semiconductor materials, the coherent coupling of a single spin on a quantum dot to a cavity hosting fermionic modes offers a new solution to this technological challenge. Here, we demonstrate coherent coupling between two spatially separated quantum dots using an electronic cavity design that takes advantage of whispering-gallery modes in a two-dimensional electron gas. The cavity-mediated, long-distance coupling effectively minimizes undesirable direct cross talk between the dots and defines a scalable architecture for all-electronic semiconductor-based quantum information processing.

Quantum information technologies emerge as a promising solution to overcome both the technological and computational boundaries that limit standard computers [1]. Quantum processing units operate with qubits—quantum bits of information. They are realized using two-level systems and take advantage of the quantum principles of superposition and entanglement of states [1–3]. These quantum properties can lead to a significant increase in our ability to solve certain types of problems, with notable examples in the fields of cryptography [4] and simulation of quantum many-body systems [5]. Building a quantum computer poses a multitude of challenges, as many components need to work together in a robust and scalable fashion. Numerous technologies are currently competing to become the leading platform for quantum information processing [6–8].

Among them, semiconductor materials offer the possibility to encode qubits using artificial atoms embedded in a two-dimensional electron gas—so-called quantum dots [9–11]. While single qubit operations via local control have been successfully implemented, 2-qubit entanglement requires a tunable coupling that is difficult to achieve. Such coupling should be scalable, noise resistant, and selective, requirements that become increasingly demanding as the density of qubits is increased [2,6–8]. Dedicated coherent systems that mediate tunable couplings between distant quantum dots offer a potential solution to these challenges. Recently, hybrid superconductor-semiconductor devices have been put forward, demonstrating coherent coupling between a quantum dot and a microwave field confined in a superconducting resonator [12–14]. Conceptually, such large-scale resonators can be used to couple spatially separated qubits.

Such a hybrid solution has to pair different technologies, and an all-electronic solution on chip is highly sought after. Short-range couplings of this type include electrostatic interaction between neighboring qubits [15] and exchange-mediated 2-qubit gates in silicon [16]. Two distant dots have been coupled by a Ruderman-Kittel-Kasuya-Yosida (RKKY) interaction in a large open dot [17] and there are further proposals for coupling distant quantum dots, e.g., via edge modes in the quantum Hall regime [18–20]. An alternative novel approach involves the introduction of an electronic cavity as a mediator of long-distance coupling: recently, such an electronic cavity that sustains coherent fermionic modes [21,22] has been strongly coupled to a quantum dot [23]. The distinct spin-coherent signatures observed in this dot-cavity setup have spurred further theoretical [24–26] and experimental [27,28] work and motivates its use as a quantum bus.

In this Letter, we demonstrate tunable coherent coupling between distant quantum dots in a mesoscopic semiconducting architecture. Using a novel kind of electronic cavity that sustains whispering-gallery modes [29,30], we achieve suppression of cross talk between the dots alongside a selective coupling mechanism. Specifically, we report on four transport spectroscopy experiments that systematically demonstrate these features. Our device can serve as a viable technological solution to the scalability challenge of semiconductor quantum information processors. At the same time, it offers a novel platform for the investigation of fascinating many-body problems in solid-state physics such as the two-impurity Kondo system [31].

Our experiments are conducted using different configurations of the device shown in Fig. 1(a). The device is cooled to an electronic temperature of ~24 mK in a dilution
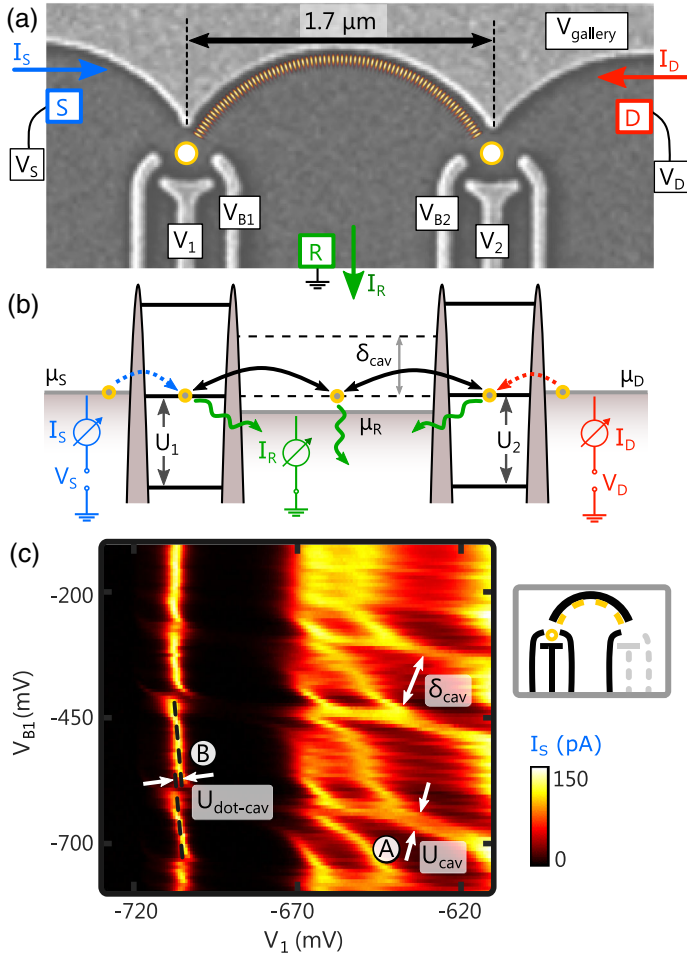
FIG. 1. (a) Scanning electron micrograph of the device; bright features are metallic top gates. Negative voltages can be applied to all the gates, with labels indicating those explicitly discussed in the text. The (yellow) circles mark the two quantum dots. A numerically calculated local density of states map (using KWANT [32]) of a whispering-gallery cavity mode close to the Fermi energy, $\varepsilon_F = 7.85$ meV is shown as an overlay. The three boxes (S), (D), and (R) label Ohmic contacts to the two-dimensional electron gas. The contact to reservoir (R) is grounded at all times, while the other two are connected to dc voltage sources. The sign of the measured currents I_S, I_D, and I_R is positive when electrons flow in the direction of the arrows. (b) Schematic energy diagram of the full dot-cavity-dot system including the confined energy levels of the two dots (black solid lines), the continuous electronic dispersion in the leads (gray boxes), and the cavity modes (black dashed lines). Full black arrows indicate coherent tunneling within the dot-cavity-dot hybrid, dotted arrows are tunneling events into either of the dots from the source or drain leads, and the wiggly green arrows represent electron relaxation to the chemical potential in the reservoir. In addition to these couplings, the different parameters of the system are the charging energies $U_1 \simeq U_2 \simeq 1$ meV of dots 1 and 2, respectively, the chemical potentials μ_α of the source, reservoir and drain ($\alpha = S, R, D$), and the cavity level spacing δ_{cav}. (c) Transport spectroscopy of the dot-cavity system (experiment I). Vertical lines correspond to transport through resonances of the left dot, while the diagonal lines are identified as cavity modes. Avoided crossings between these two sets of features are evidence of dot-cavity hybridization [23–25]. The sketch on the right indicates the gates used for this experiment. As indicated by (A), the splitting of cavity features due to its charging energy U_{cav} cannot be resolved because of the broadening of the cavity resonances. The offset indicated by (B) defines an upper bound on the dot-cavity electrostatic interaction $U_{\text{dot-cav}}$.

refrigerator. It is composed of a two-dimensional electron gas that resides 90 nm underneath the surface of a GaAs/AlGaAs heterostructure, where lithographically defined metallic top gates act as Schottky contacts. Applying suitable negative voltages depletes the underlying two-dimensional electron gas to form two spatially separated quantum dots set 1.7 μm apart from each other. Each dot is confined using three finger gates and a large arc-shaped gate (dubbed gallery). In the experiments below, we apply the same fixed voltage V_{gallery} to the gallery gate, ensuring depletion of the two-dimensional electron gas and contributing to the electrostatic definition of the dots in the few electron regime (5–10). The special feature of our device is the presence of a quasi-1D electronic cavity that sustains coherent whispering-gallery modes. These are illustrated in Fig. 1(a) using results of KWANT simulations [32] and verified by measurements of the cavity level spacing $\delta_{\text{cav}} \sim 200$ μeV, which is consistent with whispering-gallery modes (see Supplemental Material [33]), but not with radial modes [23]. These modes are embedded within the Fermi sea and modulate the local density of

states of the central reservoir; they extend between neighboring dots and hence potentially mediate their tunable coupling. Furthermore, these states are spin degenerate and devoid of charging effects due to the effective screening in the cavity. Figure 1(b) shows a schematic energy diagram of the full dot-cavity-dot system with the relevant transport processes between the setup's constituents.

Experiment I.—We demonstrate the spin-coherent coupling of the electronic cavity and the left dot. The energy of the dot is controlled by the plunger gate voltage V_1, while the cavity is defined on the left by the dot and on the right by V_{B2}, which additionally can tune the length of the cavity. We perform equilibrium transport spectroscopy of this system [34] as a function of both V_1 and V_{B2}, thus tuning the dot and cavity levels while having a small bias voltage between reservoirs (S) and (R). The result of this experiment is presented in Fig. 1(c), where we observe signatures of a competition between a dot-cavity singlet formation and Kondo transport, similar to Refs. [23,25]. This result confirms that we have successfully created a coherent fermionic cavity in a novel whispering-gallery mode
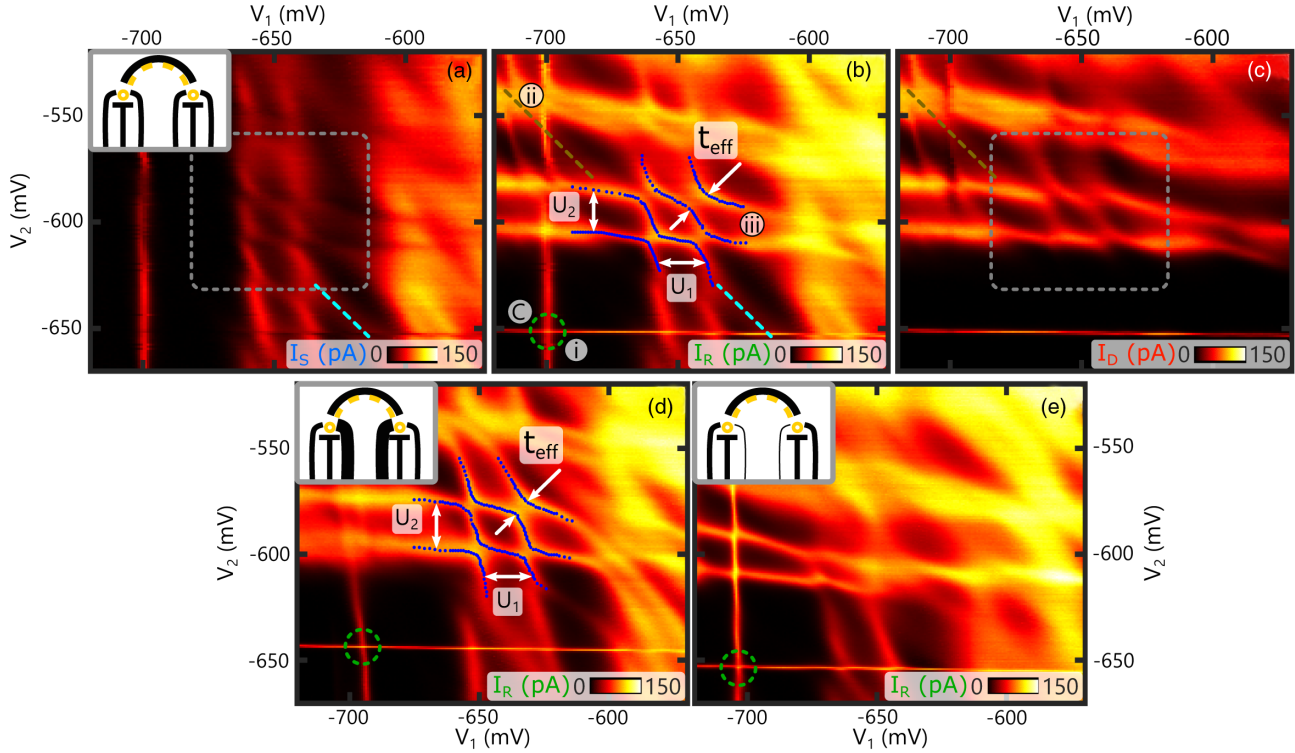
FIG. 2. (a)–(c) Spectroscopy of the dot-cavity-dot system exhibiting long-distance coupling between the two dots [experiment II; a small bias is simultaneously applied with respect to the reservoir (R) to the source (S) and drain (D) leads; the three measured currents are indicated and color coded in Fig. 1(b)]. The (gray) boxes in (a) and (c) indicate dot-cavity-dot coupling-related features, corresponding to transport category (iii) (see discussion in the text), i.e., avoided crossings between vertical and horizontal resonances. The charging energy of the two dots U_i ($i = 1, 2$) is highlighted in (b). The (blue) points correspond to the peak position of the Coulomb resonances. Several avoided crossings appear, one of them indicated by the (white) arrows, which provides the effective tunnel coupling $t_{eff} \sim 480~\mu eV$. The (green) dashed circle in the bottom-left corner belongs to transport category (i) where the two resonances associated with the left and right dot are decoupled [with the individual resonances visible in (a) and (c), respectively]. This crossing constrains the interdot charging energy to be negligibly small (C). The dashed diagonal lines refer to a transport signature of type (ii). (d),(e) Transport measurements of the same system as in experiment II, but with asymmetric tunnel barriers (experiment III). Weaker (d) and stronger (e) coupling regimes of the dot-cavity-dot hybrid are probed [symbols refer to the same quantities as in (b)]. The upper-left insets sketch which gates are active for each measurement.

geometry. Similar experiments confirm the coherent dot-cavity coupling of the second dot.

Having established the existence of an electronic cavity that can couple to our dots, we formulate a simple dot-cavity-dot model for the full device; see Fig. 1(b) [33]. Generally, electrons from each dot can (i) directly tunnel to the reservoir (R), (ii) tunnel couple independently to the cavity, forming a dot-cavity hybrid state, or (iii) form a dot-cavity-dot hybrid state with a wave function spanning both dots and the cavity; see Fig. 2 for examples of such transport signatures. Tracing out the cavity in case (iii), an effective dot-dot tunnel coupling is achieved that depends on the energetic configuration of the dot-cavity-dot system. Aligning the cavity, dot, and Fermi levels, the effective coupling is equal to the dot-cavity tunnel amplitude $t_{eff} = t_{dot-cav}$; detuning the cavity level by ε_{cav}, a perturbative analysis [33] provides the reduced effective coupling $t_{eff} \sim t_{dot-cav}^2/\varepsilon_{cav}$. Note that significantly different dot-cavity couplings for the two dots leads to case (ii) and a

suppression of t_{eff}. We show below that electrostatic interactions between electrons in different dot or cavity elements are negligible.

Experiment II.—We demonstrate the long-distance coherent coupling between the neighboring dots via the cavity. We study transport through the dot-cavity-dot system as a function of the two plunger gate voltages V_1 and V_2 and in response to a small bias voltage applied simultaneously to both source (S) and drain (D) reservoirs relative to (R). In Figs. 2(a)–2(c), the currents measured in (S), (R), and (D) are plotted, respectively. In Figs. 2(a) and 2(c), the measurement of the source (I_S) and drain currents (I_D) allows us to distinguish between the transport across the individual dots. On the other hand, the measurement of the reservoir current $I_R = I_S + I_D$ in Fig. 2(b) emphasizes the avoided crossings associated with the coherent interdot transport.

The dot-cavity-dot hybrid is modified when changing the plunger gate voltages, giving us access to all three transport
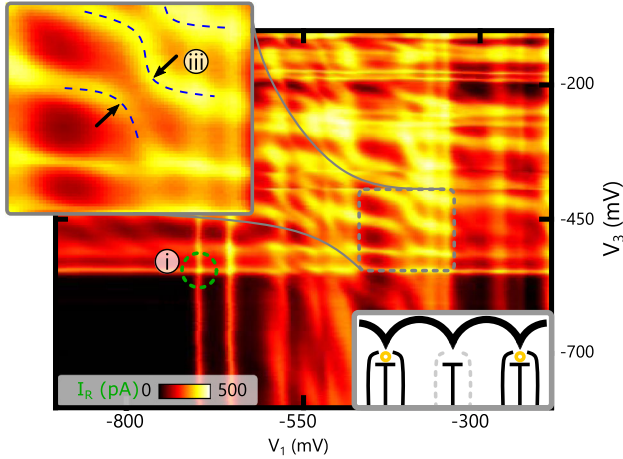
FIG. 3. Transport through a hybrid system consisting of a twice extended electronic cavity that couples next-nearest-neighbor quantum dots (experiment IV). The bottom-right inset schematically shows the gates' configuration for the experiment [33]. Similar to experiment II, we find horizontal and vertical type (i) resonances due to separate transport through the energy levels of the two dots. Avoided crossings of type (iii), appear at the intersection between specific resonances; see the magnified upper-left inset (black arrows). These are a clear signature for coherent dot-cavity-dot coupling [33]. The (blue) dashed lines are guides to the eye.

categories (i)–(iii) introduced above. Transport category (i) is clearly seen in the bottom-left corner of Fig. 2(b), where vertical (respectively, horizontal) resonance lines meet in a right angle (green dashed circle). Comparing how this feature appears in Figs. 2(a) and 2(c), we observe that the vertical (respectively, horizontal) line results from independent transport through the left (right) dot. Because of the existence of many cavity levels that couple to each of the dots independently, we observe superimposed signatures of transport category (ii); see Figs. 2(a)–2(c) and compare to Fig. 1(c). In particular, the faint diagonal resonances appearing in Fig. 2(b) (dashed lines) [23] are due to the coherent coupling of a single dot to the cavity. Comparing these features with Figs. 2(a) and 2(c), we associate them with transport exploiting the left (color) or right (color) dot-cavity hybrid, respectively.

The appearance of transport signatures that resemble a double-dot charge stability diagram [35] in all of the three measured currents is clear evidence for the strong coupling between the dots, i.e., for transport category (iii). Most importantly, this coupling is mediated by the electronic cavity, as will be further verified in experiment IV [33]. From the magnitude of the avoided-crossing gap in Fig. 2(b), we can derive the large dot-dot effective tunnel coupling $t_{\text{eff}} \sim 480\ \mu$eV.

There are three types of electrostatic interaction that potentially contribute to the size of the gaps we have associated with the dot-cavity-dot state: (A) the intracavity charging energy U_{cav}, (B) the mutual charging energy

$U_{\text{dot-cav}}$ between the dot and the cavity, and (C) the mutual dot-dot charging energy U_{12}. For the latter, the clean intersection between dot resonances, see the green dashed circles in Fig. 2(b), limits U_{12} to a pixel-wide avoided crossing of $\sim 10\ \mu$eV [36]. An upper limit for contributions (A) and (B) is obtained by further investigation of Fig. 1(c): the injection of successive electrons into the cavity only negligibly shifts the Coulomb peaks of the dot, limiting $U_{\text{dot-cav}}$ to $\sim 20\ \mu$eV; when the charging energy U_{cav} is larger than the mode's linewidth, each cavity mode should be visible as two parallel resonances separated by the Coulomb interaction. However, no clear double-peak structure is resolved in the experiment [Fig. 1(c)], and hence, we use the finite linewidth of the cavity resonances as an upper bound for $U_{\text{cav}} \simeq 30\ \mu$eV. All these contributions combined amount to at most $\sim 10\%$ of the measured coupling energy and we conclude that the gap opening is dominated by coherent tunneling. In summary, we have shown that a coherent dot-dot coupling can be mediated between distant dots using an electronic cavity [37].

It is helpful to place the measured tunnel coupling $t_{\text{eff}} \sim 480\ \mu$eV into context with (other) typical device parameters, e.g., the charging energy of the two dots $U_1 \simeq U_2 \simeq 1$ meV [highlighted in Fig. 2(b)], the dot single-particle level spacing $\sim 400\ \mu$eV, as well as coupling energies obtained in standard double-dot experiments. For the latter, typical tunnel splittings amount to $\sim 100\ \mu$eV [38], with the total coupling energy including comparable tunnel and electrostatic contributions [39,40]. The separation between the dots in the experiments of Refs. [39,40] is on the order of a few hundred nanometers, while in our sample, the distance between the dots is almost 2 μm. Hence, in spite of the larger separation between dots, the cavity-assisted coupling mechanism studied in the present Letter provides comparable effective coupling strengths between dots, with the additional advantage of a greatly suppressed electrostatic cross talk.

Experiment III.—We report on the gate tunability of our setup. We establish weak and strong coupling regimes by changing the tunnel barriers (and hence the coupling) of the dots towards the cavity via the voltages V_{B1} and V_{B2} [Fig. 1(a)]. In the weak coupling regime [Fig. 2(d)], the barriers confine the dots more strongly, resulting in narrower avoided crossings and a reduced coupling $t_{\text{eff}} \simeq 330\ \mu$eV, a $\sim 31\%$ reduction with respect to the situation in Fig. 2(b). In the strong coupling configuration [Fig. 2(e)], the reduced confinement of the dots washes out the signatures of strong dot-cavity-dot hybridization that was observed in Fig. 2(c). The coupling between the dots and the cavity increases to the point where we expect the system to behave more like a single quantum dot with a large area, instead of three separated (but coupled) systems. Experiment III offers a path towards achieving complete on-off switching of the coupling with future improved designs.

Experiment IV.—We test the potential of the cavity-mediated coupling to extend over longer distances. Taking advantage of a third dot present in our sample [33], we repeat experiment II with a next-nearest-neighbor configuration (see lower inset in Fig. 3). The dots in this case reside 3.5 μm apart from each other and are coupled via a whispering-gallery mode spanning two cavity arcs; the gate controlled by V_2 partially depletes the central reservoir without forming a dot and connects the two cavities [33]. In Fig. 3, we observe avoided crossings characteristic of transport category (iii), as highlighted in the upper inset. Along with measurements of the individual source and drain currents [33], we obtain clear evidence of a dot-dot cavity-mediated tunnel coupling. The splitting is observed only when the two-arc gallery mode is formed, i.e., when the gate bias V_2 is properly tuned [33], thus providing a further tuning parameter to switch the interdot coupling on and off.

The long-distance, cavity-mediated tunnel coupling between dots investigated in our device offers an all-electronic controllable platform for quantum information processing. In particular, the reduced electrostatic cross talk and the tunable long-distance coherent coupling provide a possible solution to the scalability challenges in semiconducting architectures. Further improvements of our prototypical cavity design may offer higher control and selective connectivity and thus the possibility of entanglement experiments with two or more qubits [41,42]. Furthermore, our system can be used to study many-body physics phenomena, such as exotic Kondo systems involving two magnetic impurities, i.e., two isolated spins confined in the dots [31] and the competition between cavity-assisted and RKKY-mediated coupling [17], as well as the realization of a potential Kondo-cat state [25].

[1] M. A. Nielsen and I. L. Chuang, *Quantum Computation and Quantum Information*, 10th ed. (Cambridge University Press, Cambridge, England, 2010).

[2] D. Loss and D. P. DiVincenzo, Phys. Rev. A **57**, 120 (1998).

[3] J. Clarke and F. K. Wilhelm, Nature (London) **453**, 1031 (2008).

[4] P. Shor, SIAM Rev. **41**, 303 (1999).

[5] D. S. Abrams and S. Lloyd, Phys. Rev. Lett. **79**, 2586 (1997).

[6] M. H. Devoret and R. J. Schoelkopf, Science **339**, 1169 (2013).

[7] D. D. Awschalom, L. C. Bassett, A. S. Dzurak, E. L. Hu, and J. R. Petta, Science **339**, 1174 (2013).

[8] D. Rotta, F. Sebastiano, E. Charbon, and E. Prati, npj Quantum Inf. **3**, 26 (2017).

[9] T. Hayashi, T. Fujisawa, H. D. Cheong, Y. H. Jeong, and Y. Hirayama, Phys. Rev. Lett. **91**, 226804 (2003).

[10] J. Gorman, D. G. Hasko, and D. A. Williams, Phys. Rev. Lett. **95**, 090502 (2005).

[11] J. R. Petta, A. C. Johnson, J. M. Taylor, E. A. Laird, A. Yacoby, M. D. Lukin, C. M. Marcus, M. P. Hanson, and A. C. Gossard, Science **309**, 2180 (2005).

[12] L. E. Bruhat, T. Cubaynes, J. J. Viennot, M. C. Dartiailh, M. M. Desjardins, A. Cottet, and T. Kontos, arXiv:1612.05214.

[13] A. Stockklauser, P. Scarlino, J. V. Koski, S. Gasparinetti, C. K. Andersen, C. Reichl, W. Wegscheider, T. Ihn, K. Ensslin, and A. Wallraff, Phys. Rev. X **7**, 011030 (2017).

[14] X. Mi, J. V. Cady, D. M. Zajac, P. W. Deelman, and J. R. Petta, Science **355**, 156 (2017).

[15] M. D. Shulman, O. E. Dial, S. P. Harvey, H. Bluhm, V. Umansky, and A. Yacoby, Science **336**, 202 (2012), http://science.sciencemag.org/content/336/6078/202.full.pdf.

[16] M. Veldhorst, C. H. Yang, J. C. C. Hwang, W. Huang, J. P. Dehollain, J. T. Muhonen, S. Simmons, A. Laucht, F. E. Hudson, K. M. Itoh, A. Morello, and A. S. Dzurak, Nature (London) **526**, 410 (2015).

[17] N. J. Craig, J. M. Taylor, E. A. Lester, C. M. Marcus, M. P. Hanson, and A. C. Gossard, Science **304**, 565 (2004).

[18] S.-R. E. Yang, J. Schliemann, and A. H. MacDonald, Phys. Rev. B **66**, 153302 (2002).

[19] V. W. Scarola, K. Park, and S. D. Sarma, Phys. Rev. Lett. **91**, 167903 (2003).

[20] S. J. Elman, S. D. Bartlett, and A. C. Doherty, Phys. Rev. B **96**, 115407 (2017).

[21] J. A. Katine, M. A. Eriksson, A. S. Adourian, R. M. Westervelt, J. D. Edwards, A. Lupu-Sax, E. J. Heller, K. L. Campman, and A. C. Gossard, Phys. Rev. Lett. **79**, 4806 (1997).

[22] J. S. Hersch, M. R. Haggerty, and E. J. Heller, Phys. Rev. Lett. **83**, 5342 (1999).

[23] C. Rössler, D. Oehri, O. Zilberberg, G. Blatter, M. Karalic, J. Pijnenburg, A. Hofmann, T. Ihn, K. Ensslin, C. Reichl, and W. Wegscheider, Phys. Rev. Lett. **115**, 166603 (2015).

[24] M. S. Ferguson, C. Rössler, T. Ihn, K. Ensslin, G. Blatter, and O. Zilberberg, arXiv:1612.03850.

[25] M. S. Ferguson, D. Oehri, C. Rössler, T. Ihn, K. Ensslin, G. Blatter, and O. Zilberberg, Phys. Rev. B **96**, 235431 (2017).

[26] L. G. G. V. Dias da Silva, C. H. Lewenkopf, E. Vernek, G. J. Ferreira, and S. E. Ulloa, Phys. Rev. Lett. **119**, 116801 (2017).

[27] C. Yan, S. Kumar, M. Pepper, P. See, I. Farrer, D. Ritchie, J. Griffiths, and G. Jones, Phys. Rev. Applied **8**, 024009 (2017).

[28] R. Steinacher, C. Pöltl, T. Krähenmann, A. Hofmann, C. Reichl, W. Zwerger, W. Wegscheider, R. Jalabert, K. Ensslin, D. Weinmann *et al.*, arXiv:1709.08559.

[29] C. V. Raman and G. A. Sutherland, Nature (London) **108**, 42 (1921).

[30] Y. Zhao, J. Wyrick, F. D. Natterer, J. F. Rodriguez-Nieva, C. Lewandowski, K. Watanabe, T. Taniguchi, L. S. Levitov, N. B. Zhitenev, and J. A. Stroscio, Science **348**, 672 (2015).

[31] A. M. Chang and J. C. Chen, Rep. Prog. Phys. **72**, 096501 (2009).

[32] C. W. Groth, M. Wimmer, A. R. Akhmerov, and X. Waintal, New J. Phys. **16**, 063065 (2014).

[33] See Supplemental Material at http://link.aps.org/supplemental/10.1103/PhysRevLett.120.236801 for (i) information on sample fabrication and characterization, (ii) additional data on the tuning of the cavity-mediated coupling and (iii) a theoretical description of electronic cavities and the dot-cavity-dot hybrid.

[34] C. Rössler, S. Burkhard, T. Krähenmann, M. Röösli, P. Märki, J. Basset, T. Ihn, K. Ensslin, C. Reichl, and W. Wegscheider, Phys. Rev. B **90**, 081302 (2014).

[35] W. G. van der Wiel, S. De Franceschi, J. M. Elzerman, T. Fujisawa, S. Tarucha, and L. P. Kouwenhoven, Rev. Mod. Phys. **75**, 1 (2002).

[36] T. Ihn, *Semiconductor Nanostructures: Quantum States and Electronic Transport* (Oxford University Press, New York, 2010).

[37] Even though the cavity-mediated strong coupling between dots can be explained both by spinful and spinless models, several indications support the spinful case: the dot-cavity coupling (experiment I) exhibits spin-coherent coupling between a dot and a set of cavity levels with spacing ~ 200 μeV; in the double-dot case (experiment II), the cavity signatures appear with similar spacing [Figs. 2(a)–2(c)], which suggest that the same set of cavity states is responsible for the coupling observed in experiments I and II.

[38] R. H. Blick, D. Pfannkuche, R. J. Haug, K. v. Klitzing, and K. Eberl, Phys. Rev. Lett. **80**, 4032 (1998).

[39] T. Hatano, M. Stopa, T. Yamaguchi, T. Ota, K. Yamada, and S. Tarucha, Phys. Rev. Lett. **93**, 066806 (2004).

[40] T. Hatano, M. Stopa, and S. Tarucha, Science **309**, 268 (2005).

[41] S. Mehl, H. Bluhm, and D. P. DiVincenzo, Phys. Rev. B **90**, 045404 (2014).

[42] V. Srinivasa, H. Xu, and J. M. Taylor, Phys. Rev. Lett. **114**, 226803 (2015).